Automatic Grinder Based on Ansys-Workbench

Base structure optimization design

Abstract: In order to solve the problem that the various devices on the base of an automatic grinding machine are deformed and the static performance changes due to their own gravity, the three-dimensional modeling of the base of the automatic grinding machine is carried out and imported into Workbench for static analysis. Based on the static analysis, topology optimization is carried out to optimize the base structure to achieve the lightweight design and performance improvement of the automatic grinder base. Through topology optimization and analysis of cloud map and actual working conditions, two structural optimization schemes are proposed. Finally, through static analysis of the two optimization schemes, the feasibility of the scheme is verified and its advantages and disadvantages are compared, and the automatic grinding machine base is obtained. The optimal structure optimization scheme, the weight of the optimized base is reduced by 11.6%.

Key words: automatic grinder base; structural optimization design; topology optimization; static analysis

INTRODUCTION

Graphite has been widely used in the manufacture of molds in industrial production in recent years due to its excellent thermal and electrical conductivity, lubricating properties, and its characteristics that it is not easy to corrode and does not chemically react with other metal materials. Graphite molds are often used in hot-pressed sintered diamond tools. For example, in the production of polycrystalline diamond tools (PCD tools), the quality of graphite molds will greatly affect the accuracy of PCD tools. There are many processing technologies for graphite molds. High-precision grinding of each surface by an automatic grinding machine is an efficient and accurate processing technology used in factories at this stage.

Grinding is an indispensable key technology in the optoelectronic industry and advanced processing and manufacturing technology industry. The emergence of automatic grinding machines has largely solved some of the possible problems of precision, cost and quality in traditional grinding technology. The base is all kinds of machine tools and their important bearing parts. The automatic grinding machine proposed in this paper includes mechanical arms, double-end grinders, servo motors, etc. Due to the influence of its own gravity, the structure of the base will be greatly deformed. In order to ensure the overall structure of the grinding machine The safety and light weight of the design are used to reduce the deformation hazards caused by gravity, and the base structure is optimized for various unsteady phenomena that may

occur during the actual grinding process of the mold. The purpose of the optimized design is mainly two aspects, one is to reduce the mass of the grinder base to achieve a lightweight design and reduce the deformation of the base structure caused by gravity, and the other is to improve the ability of the grinder base to resist deformation due to gravity as much as possible. its security.

In this paper, Solid Works is used to model the base of the automatic grinding machine, and the base model is imported into Workbench for static analysis, and the base structure is optimized through the Topology optimization module in Workbench. Carry out the optimization design, and perform static analysis again on the results after the optimization design to check whether the optimized structure is reasonable.

1 Automatic grinding machine base structure

The automatic grinding machine includes a grinding device, a main power mechanism, a positioning mechanism and an automatic loading and unloading device. The main power mechanism uses a servo motor to drive the synchronous belt to work on the guide rail. As shown in Figure 1, when the workpiece arrives at the station with the synchronous belt, in order to ensure the accuracy of grinding, there will be a cam follower to position the workpiece. As shown in Figure 2, the grinding device uses an end face grinder mechanism to grind the side surface of the workpiece.

As shown in Figure 3, the automatic loading and unloading device uses the SCARA robotic arm to transport the workpiece. The SCARA robotic arm (Selective Compliance Assembly Robot Arm) is a horizontal multi-joint robotic arm. It is a four-axis robotic arm commonly used for loading and unloading in industrial production. The four independent drive joints include three rotating joints with parallel axes and one moving joint. The functions of orientation and positioning are realized by 3 rotary joints, and linear motion is completed by moving joints. Because of its simple structure, it can be better used in fast movement, so it is suitable for fast sorting.

After the workpiece is put into the carrier by the SCARA robot arm, the workpiece is processed with the conveyor belt. When the workpiece is ground, the workpiece is taken out of the carrier by the robot arm and put into the conveyor line, and sent out with the conveyor line.

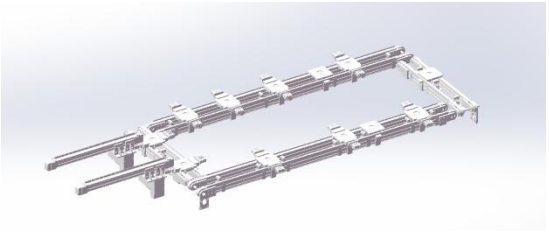

Figure 1 Timing belt guide

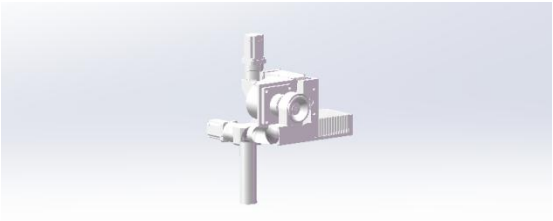

Figure 2 Side Grinder Mechanism

Figure 3 SCARA Robotic Arm

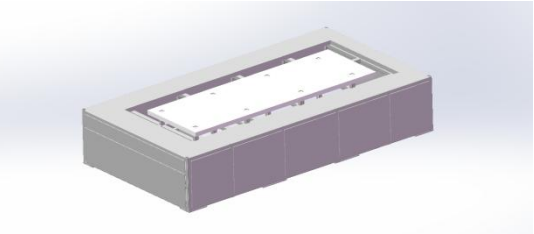

Figure 4 Grinder Base

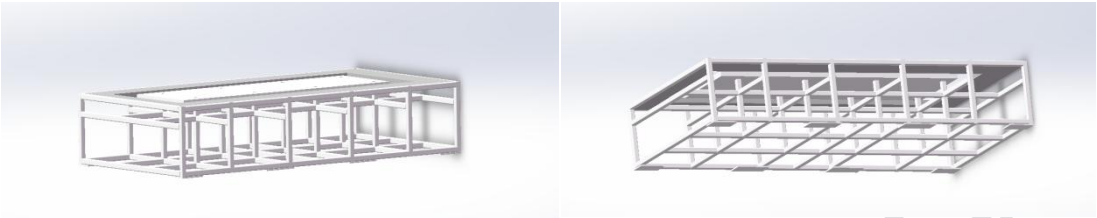

Figure 5 Base frame

The base of the automatic grinder is shown in Figure 4. The synchronous belt guide rail is installed between the two working planes of the base. The two working planes are equipped with a side grinder mechanism, a tightening mechanism and a rotating mechanism. The mechanical arm for loading and unloading is placed in the product input. line and output line. In order to facilitate a clearer observation of the frame analysis inside the base in the subsequent Workbench, the baffles in the base are hidden for static analysis. The internal frame structure of the base is shown in Figure 5, and then the base frame model drawn by Solid works is saved. Import into Workbench Static Analysis module for x.t format. The base material of the automatic grinder is HT300, and Table 1 shows the material parameters of the base.

Material	Poisson's ratio	Elastic Modulus /MPa	density /(kg*m^{-3})	Yield Strength /MPa
HT300	0.25	1.3×10^5	7300	300

Table 1 Base material parameters

2 Static analysis of base structure

2.1 Theoretical basis of static analysis

The theoretical basis of static analysis can be derived from classical mechanics. According to classical mechanics, the generalized dynamic equilibrium equation for solving the structure in ANSYS is:

$$[M]\{\ddot{x}\} + [C]\{\dot{x}\} + [K]\{x\} = \{F(t)\}\#(2-1)$$

In the formula, [M] is the mass matrix; [C] is the damping matrix; [K] is the stiffness matrix; {x} is the displacement vector, F(t) is the total external force, and the static analysis mainly studies the effect of constant external load The mechanical response under , usually, without considering inertia and damping factors, in the linear static analysis, the quantity related to time t is removed, so equation (2-1) is simplified to:

$$[K]\{x\} = \{F\}\#(2-2)$$

The nodal displacements are obtained according to the known loads and boundary conditions, and then the stress-strain and other results are obtained according to the nodal displacements.

2.2 Base mesh division

Before starting the static analysis, import the base model established by Solid Works and set the material parameters before meshing. The fineness of meshing affects the results of the simulation analysis to a large extent. It can achieve more accurate simulation results as much as possible under high computing power, and reduce the errors that may occur during complex long-term meshing. , which are divided into 512,905 nodes and 273,307 units.

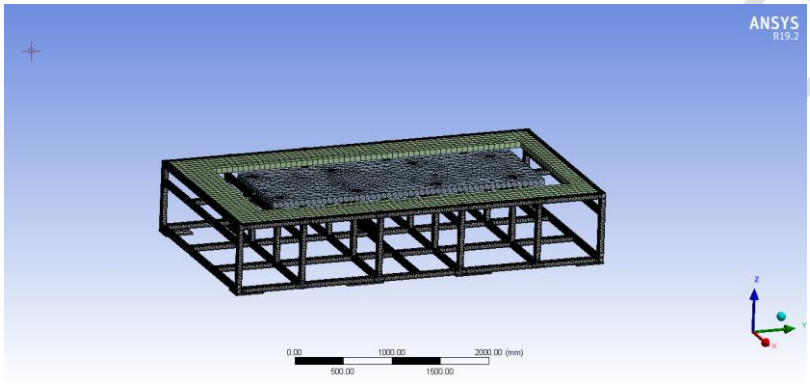

Figure 6 Meshing

2.3 Static analysis results of the base

The gravity of the synchronous belt guide rail, positioning mechanism, grinder, SCARA robot arm, bearing, mold, etc. that the grinder base bears is about 35KN, and then the gravity constraint is applied to the grinder base, and the fixed constraint is the lower bottom surface of the base frame. Click Solve to perform a static analysis. After the load is applied, the base of the grinder is deformed to a certain extent. The strain cloud diagram and equivalent stress diagram of the base are shown in Figure 7 and Figure 8.

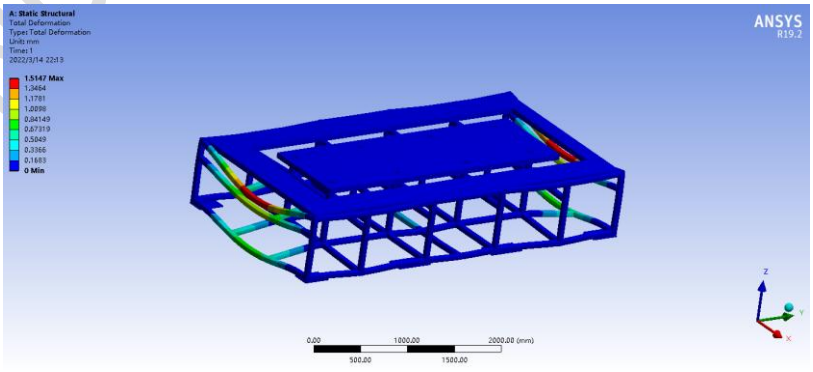

Fig.7 Strain cloud diagram of the base of automatic grinding machine

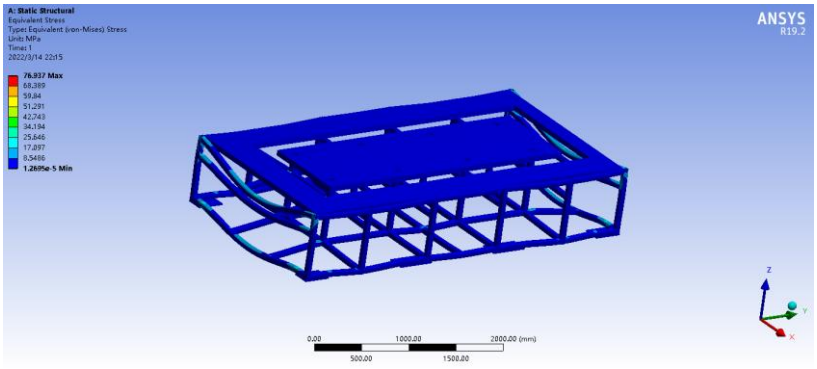

Figure 8 Equivalent stress cloud map

It can be seen from the strain cloud diagram of the base in Figure 8 that the maximum deformation of the base of the automatic grinding machine is on both sides of the base frame, and the maximum deformation of the base frame is 1.5147mm, which is much smaller than the allowable deformation error. It can be seen from Figure 8 that the maximum equivalent stress of the base of the grinder is 76.937MPa, which is still much different from the yield strength of HT300, which is 300Mpa. The base fatigue fracture will not occur. The structure of the base frame meets the design requirements, and the base of the grinder does not need to be considered. Therefore, there is still room for weight reduction and optimization of the grinder base.

3 Optimum design of base structure

3.1 Principle of topology optimization

The method of calculating the optimal distribution ratio of materials in the three-dimensional space of an object by the general numerical analysis method is topology optimization. In the case of normal transfer between structures, the structure of the entity is optimized, that is, an appropriate number of entity areas are subtracted, for example, some holes are added to the interior of the entity to achieve the best matching form. Compared with general shape or size optimization, the biggest advantage of topology optimization is that it has a high degree of freedom. Designers can use the analysis results of topology optimization to carry out various optimization design schemes for the target object.

Commonly used methods for topology optimization include homogenization method, variable density method, progressive structure optimization (ESO), level set method, and moving morphable void (MMV) method. Compared with other methods, the variable density method has faster calculation efficiency and higher precision, and can be more easily implemented by programs. The principle of the variable density method is to find the optimal force transmission route through the density function of continuous variables, which can explicitly express the corresponding relationship between the relative density and elastic modulus of material units. SMIP is selected as the material interpolation model of variable density method.

The basic idea of SIMP is to discretize the continuum based on the finite element, and establish a nonlinear functional relationship between the elastic modulus and the relative density of the element by introducing the element design variables that change continuously in the 0-1 interval. The removal and retention of cells is determined according to the value of cell density. The commonly used material interpolation models based on the SIMP format are:

$$E_i = E(i) = {x_i}^P E_0, x_i \in [0,1] \quad (3\text{-}1)$$

In the formula, $E_i$represents the elastic modulus of the i-th element, x_i represents the relative density of the i-th element (1 represents a solid element, 0 represents an empty element), E_0 represents the elastic modulus of the solid material, and P is the penalty coefficient. The purpose is to Make intermediate density values between 0 and 1 tend towards 0 or 1, thereby reducing intermediate variables.

Since the finite element analysis may have the singularity problem of the stiffness matrix, in order to avoid this problem, a small non-negative E_{min} is used as the elastic modulus of the empty element to improve the original model. Improved SIMP interpolation Model is:

$$E_i = E(x_i) = E_{min} + x_i^p(E_0 - E_{min}), x_i \in [0,1] \#(3-2)$$

Generally, $E_{min} = E_0/1000$ is set. According to the Hashin-Shtrikman boundary conditions, the SIMP material mode should meet the following conditions:

$$\begin{cases} 0 \le \dfrac{{x_i}^P E_0}{2(1-v_0)} \le \dfrac{x_i E_0}{4-2(1+v_0)x_i} \\ 0 \le \dfrac{{x_i}^P E_0}{2(1-v_0)} \le \dfrac{x_i E_0}{2(1-x_i)(3-v_0)+2(1+v_0)} \end{cases} \#(3-3)$$

The penalty factor P that can be calculated by formula (3-3) needs to meet the following conditions:

$$P \ge P*(v_0) = max\left\{\frac{2}{1-v_0}, \quad \frac{4}{1+v_0}\right\} \#(3-4)$$

In the SIMP material interpolation model, the control parameters of the element elastic modulus are x_i and P, and the degree of penalty for the intermediate value density will change continuously with the value of the element elastic modulus P value. At -0 or E_0, the material selection will be completed to achieve the function of topology optimization.

3.2 Base topology optimization process and results

Perform topology optimization analysis on the base of the grinder, select the Topology Optimization module, and associate the static analysis results obtained earlier with this module, set the maximum number of iteration steps to 500, and the convergence accuracy to 0.001. Through the optimal iteration algorithm, when the maximum Stop the iteration after the number of iterations or the optimal iteration accuracy, and calculate the result after topology

optimization. The results of topology optimization show that there are two density units, 0 and 1. The size of the density value represents the influence of the position on the structure. When the value is smaller, the influence on the structure is smaller, and vice versa.

The final optimization result is shown in Figure 9. The red part in the figure is between 0 and 0.4, which is the area where this part of the material can be removed, the yellow area is between 0.4 and 0.6, which is the critical area, and the gray area is the density of 0.6. Between 1.0, it is the area where this part of the material can be retained. According to the experience and the special needs of actual production, delete and correct the materials in the red area and the yellow area or redesign part of the structure in this area to achieve the best structural requirements suitable for production needs. After the structural optimization of topology optimization is completed , the static analysis of the new base structure is carried out to verify the feasibility of the optimization.

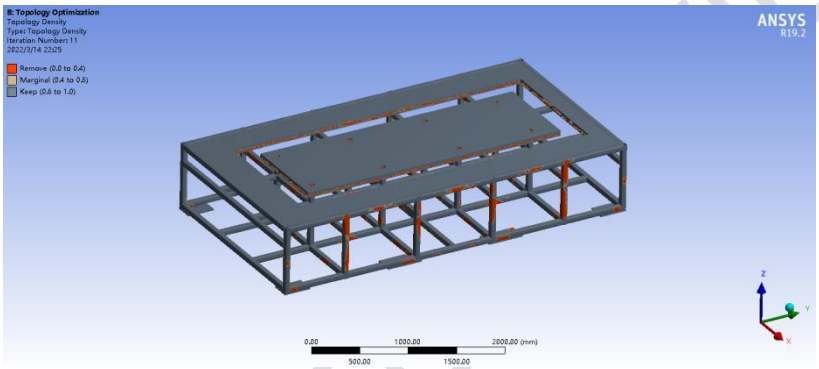

Figure 9 Cloud diagram of topology optimization analysis

3.3 Optimization scheme of base structure

According to the cloud diagram of the base topology optimization analysis, the structural optimization design scheme can start from improving the internal frame structure of the base and reducing the thickness of the two working planes. In order to ensure the rationality of the optimization scheme, not only the weight of the base should be reduced, but also the strength of the base must be guaranteed. , and the structural change of the base frame will affect the strength of the overall base, so if the base frame is optimized, it is necessary to pay attention to the change of the overall base strength. Changes to the base frame structure.

As shown in Figure 10, for the first optimization design scheme, the base structure of the automatic grinder is redesigned according to the topological optimization analysis cloud diagram. It can be seen that the material of the base frame has little effect on the overall strength of the base, so by adjusting this The material of part of the base frame is appropriately reduced to achieve the overall weight reduction of the base.

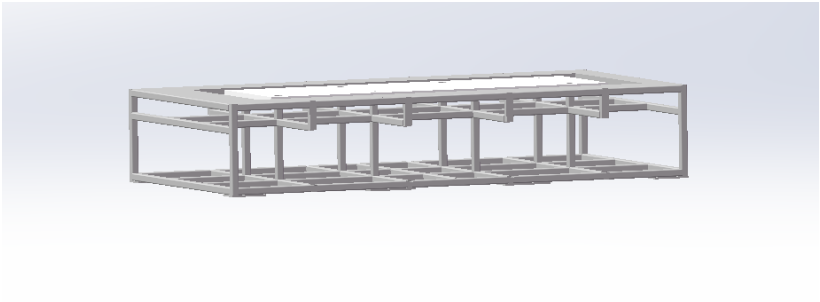

Figure 10 Scheme 1

As shown in Figure 11, for the second optimal design scheme, the red and yellow areas of the cloud map are analyzed according to topology optimization, and the thickness of the two working planes is optimized. Secondly, in order to ensure the connection between the optimized working plane and the base frame The tightness makes the whole base have sufficient strength, reduces the strain of the base, and changes the contact mode between the two working planes and the base frame, so that the lower surfaces of the two working planes and the base frame are bound and contacted together.

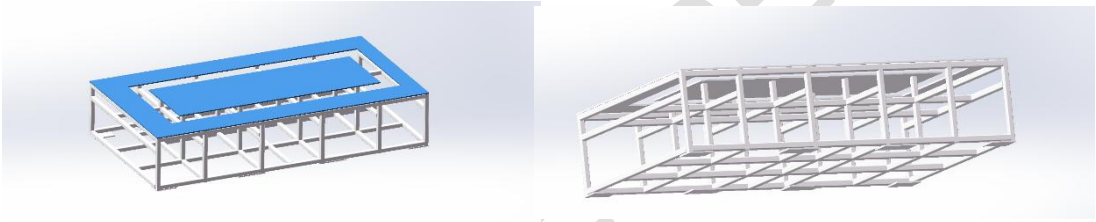

Figure 11 Scheme 2

4 Verification of the optimization scheme of the base frame

In order to verify whether the two optimization schemes are reasonable, import the 3D models of the optimization scheme 1 and the optimization scheme 2 into the Workbench for static analysis again, analyze the statics results and verify the rationality of the scheme, and at the same time, according to the advantages and disadvantages of the before and after optimization effects , compare the advantages and disadvantages of the two schemes, and choose the most reasonable base optimization scheme.

The static analysis results of the optimization scheme 1 are shown in Figure 11 and Figure 12. The maximum deformation of the optimized base occurs in the center of the base frame after the material is subtracted, which is 1.6459mm, although it is also within the allowable amount of the automatic grinding machine base. Within the maximum displacement error range, but compared with before optimization, the maximum deformation is increased and the deformation area is also larger. The maximum equivalent stress of the base is 100.03Mpa, which is still worse than the yield strength of the base material HT300. There are many, so the optimized base strength is in line with the requirements.

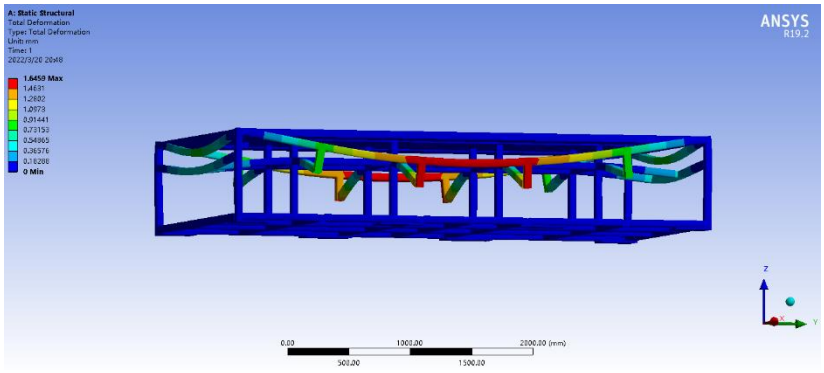

Figure 12 Strain cloud diagram of scheme 1

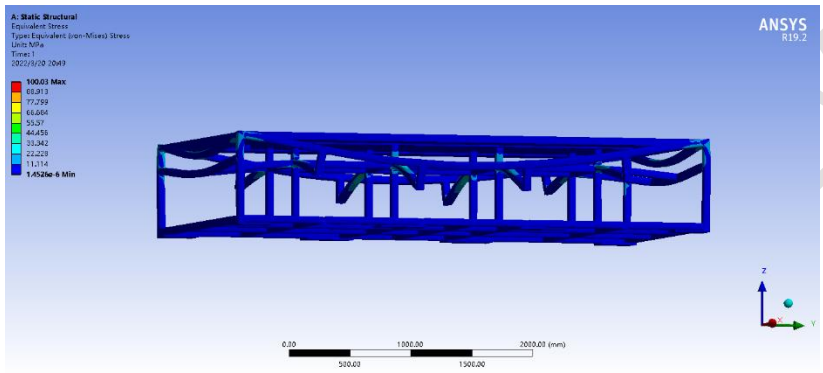

Figure 13 Scheme 1 Equivalent stress

The static analysis results of the optimization scheme 2 are shown in Figure 14 and Figure 15. At this time, it can be seen from the strain cloud diagram and equivalent stress cloud diagram of the scheme 2 that the part with the largest deformation of the base frame is the same as before the optimization. , but the deformation area is much less than before optimization. The maximum deformation of the optimization scheme 2 is 0.96515mm, which is smaller than that before the optimization and scheme 1, and the maximum equivalent stress of the base is 49.492Mpa, which also meets the yield strength requirements of the base material.

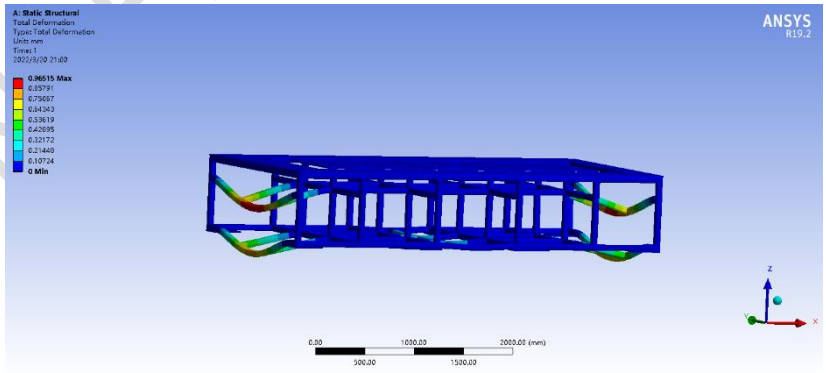

Fig. 14 Strain cloud diagram of scheme

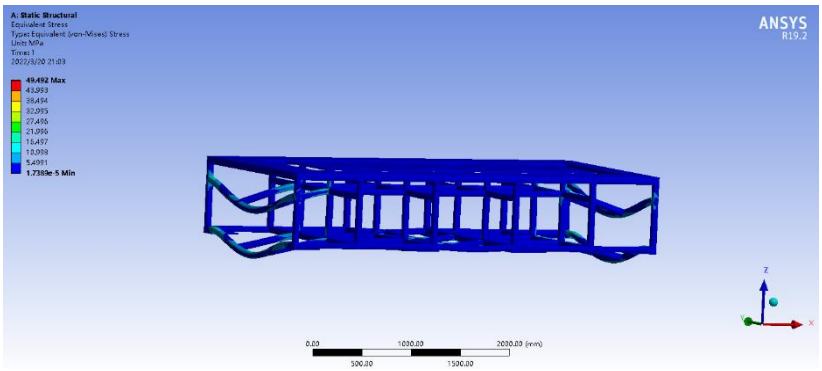

Fig. 15 Equivalent stress cloud diagram of scheme 2

Based on the above analysis, it can be seen that the weight of Scheme 1 is reduced by 16.7% on the original basis, the maximum deformation is increased by 8.7%, and the maximum equivalent stress is increased by 30.01%; The amount of deformation is reduced by 36.3%, and the maximum equivalent stress is reduced by 35.7%. The optimization scheme 1 achieves the optimal weight reduction effect, but at the same time, the deformation of the base increases and the deformed area also becomes larger. Compared with the optimization scheme 2, although the weight reduction effect is inferior to the scheme 1, the base The overall strain and stress have been improved to better ensure the strength of the base. The weight of the automatic grinder base optimized by scheme 2 significantly reduces the strain and maximum stress, and achieves the goal of better base structure optimization. Therefore, scheme 2 is finally selected to optimize the base.

5 Conclusion

In this paper, the three-dimensional model of the automatic grinding machine base is established through Solid Works. First, the static analysis of the base is carried out, and the stress and strain results are analyzed to confirm that it meets the design standards. Use Workbench topology optimization module to optimize the structure of the base, carry out preliminary optimization design of the base according to the cloud diagram of the topology optimization analysis of Workbench, make small changes to the base structure, and propose two different optimization schemes, and carry out static analysis of the two schemes To verify the feasibility of the scheme, and compare and analyze the advantages and disadvantages of the two schemes, the static analysis cloud diagram shows that the optimization scheme 2 reduces the strain and maximum stress while reducing the weight by 11.6%, and realizes the lightweight design of the automatic grinder base. The comprehensive performance of the automatic grinding machine has been improved.

References:

[1] Chu Fei, Lei Yu, Gao Han. Topology optimization design of the connecting plate on the lifting ring side of the top drive based on ANSYS Workbench [J] Mechanical Design and Research, 2019, 35(01): 189-191+195.
[2] Yan Gaochao, Shen Xiaoqin, Yu Fusheng. Optimization design of underwater robot frame structure based on ANSYS-Workbench [J] Manufacturing Automation, 2020, 42(10): 1-3+7.
[3] Zhou Bing, Huang Yi, Yang Guangyou. Analysis and optimization of battery packer positioning mechanism based on Workbench [J] Manufacturing Automation, 2015, 37(02): 45-46+52.
[4] Zhai Hongfei, Hou Junjian, Fang Zhanpeng. Research on lightweight in-wheel motor housing structure based on topology optimization [J] Mechanical Design, 2022, 39(01): 105-110.
[5] Lu Cunzhuang, Yu Luchuan, Zhang Jianhua. Structural design of scallop shelling machine based on topology optimization [J] Mechanical Design, 2021, 38(12): 7-11.
[6] Wang Yan, Zhou Caicai, Zhou Yan, Wang Bo. Design of aero-engine lubricating oil tank bracket based on topology optimization [J] Propulsion Technology, 2022, 43(02).
[7] Liu Jinlei, Zhu Nanhai. Lightweight design of H-beam web section based on topology optimization [J] Chinese Journal of Applied Mechanics, 2021, 38(06).
[8] Wan Yipin, Jia Jie, Ma Zhining. Mechanical analysis and topology optimization design of loader arm structure [J] Mechanical Design, 2021, 38(12).
[9]Masatoshi Shimoda, Shoki Tani.Simultaneous shape and topology optimization method for frame structures with multi-materials[J] Structural and Multidisciplinary Optimization，2021.：1-22.
[10] Yichang Liu, Mingdong Zhou,Chuang Wei,Zhongqin Lin. Topology optimization of self-supporting infill structures [J] Structural and Multidisciplinary Optimization，2021:1-16.
[11] Yuang Liang,Kai Sun,GengDong Cheng. Discrete variable topology optimization for compliant mechanism design via Sequential Approximate Integer Programming with Trust Region (SAIP-TR)[J] Structural and Multidisciplinary Optimization，2020，62：1-29.
[12]Jun Zou, Yuechao Zhang, Zhenyu Feng. Topology optimization for additive manufacturing with self-supporting constraint[J] Structural and Multidisciplinary Optimization，2021：1-13.
[13]Jannis Greifenstein,Michael Stingl. Topology optimization with worst-case handling of material uncertainties[J] Structural and Multidisciplinary Optimization，2020,61:1-21.
[14] Eddie Wadbro, Bin Niu. Multiscale design for additive manufactured structures with solid coating and periodic infill pattern[J] Computer Methods in Applied Mechanics and Engineering,2019,357:112605-112605.

[15]Han Yongsheng,Xu Bin,Wang Qian,Liu Yuanhao, Duan Zunyi. Topology optimization of material nonlinear continuum structures under stress constraints[J] Computer Methods in Applied Mechanics and Engineering,2021,378:113731-113731.
[16] Casper Schousboe Andreasen. A framework for topology optimization of inertial microfluidic particle manipulators[J] Structural and Multidisciplinary Optimization, 2020,61:1-19.